The high-temperature paramagnetic susceptibility of the system $(Fe_{1-x}Mn_x)_2P$

1989 J. Phys.: Condens. Matter 1 9599

(http://iopscience.iop.org/0953-8984/1/48/010)

J. Phys.: Condens. Matter 1 (1989) 9599–9607. Printed in the UK

The high-temperature paramagnetic susceptibility of the system $(Fe_{1-x}Mn_x)_2P$

B Chenevier†, D Fruchart‡, M Bacmann‡, D Boursier† and R Fruchart†

† Laboratoire des Matériaux et du Génie Physique, UA 1109, ENSPG, BP 46, 38402 Saint-Martin d'Hères, France

‡ Laboratoire de Cristallographie, CNRS, associé à l'Université Joseph Fourier 166X, 38042 Grenoble Cédex, France

Received 28 March 1989, in final form 14 June 1989

Abstract. For the system $(Fe_{1-x}Mn_x)_2P$ $(0 \leqslant x \leqslant 1)$, numerous previous studies have shown that Fe- and Mn-rich solid solutions crystallise with a hexagonal symmetry (H) and intermediate compositions are of orthorhombic type (O). The H and O phases are those generally encountered in the transition-metal pnictides of formula MM'X (M, M': transition metal; X: P or As). Analysis of the paramagnetic state at the highest temperatures reveals the stability of the H structure for the whole system. The magnetic transition observed at high temperature for intermediate ranges of composition can be related to the crystal O ↔ H transformation already observed by neutron diffraction. In most of the cases, a metastable hexagonal phase can be retained by ensuring fast quenching. A complete phase diagram, versus composition and temperature, is proposed. The reciprocal paramagnetic susceptibility behaviour as temperature is varied provides evidence for large magnetic correlations far above the ordering temperature for the hexagonal form only. For a given composition, a strong influence of the local metal environment on the magnetic couplings is thus emphasised for both H and O forms of the MM'X series.

1. Introduction

The transition-metal pnictides with general formula MM'X (M, M': transition metal; X: P or As) are well known to crystallise generally in one of the three related structure types Co_2P (space group $Pnma$), Fe_2P (space group $P\bar{6}2m$) and Fe_2As (space group $P4/nmm$) [1–4]. The nearest neighbours of the metal atoms are X atoms. The metal environments in the X atoms are tetrahedra and square-based pyramids.

The crystallographic and magnetic properties of the Fe_2P–Mn_2P system have been studied intensively in the last few years [5–9]. From the studies it is found that at room temperature the crystal structures are of orthorhombic symmetry (O) for compositions in the range $0.25 \leqslant x \leqslant 0.70$ and of hexagonal symmetry (H) for the other compositions [6]. A marked tendency for the Mn atoms selectively to occupy the pyramidal sites has also been reported. The compounds exhibit ordered magnetic states with critical temperatures located below 300 K. A very small substitution ($x \geqslant 0.02$) for Fe with Mn transforms the ferromagnetic behaviour of Fe_2P [8]. When the degree of substitution is increased, a long-period antiferromagnetic structure appears. In the orthorhombic

0953-8984/89/489599 + 09 $02.50

intermediate range, the compounds are antiferromagnetic with the maximum critical temperature exhibited by FeMnP [6]. For $x \geqslant 0.70$, the hexagonal compounds show magnetic structures directly related to that of Mn_2P [10]. Pyramidal sites share the largest magnetic moment ($\simeq 3.0\ \mu_B$). The existence of a small magnetic moment on the tetrahedral sites was also detected [6, 10–12].

In a recent paper [13], a high-temperature crystal transformation has been reported for FeMnP. This transition associated with a hysteresis phenomenon was studied by neutron diffraction. Above 1413 K, the compound was shown to be of the hexagonal Fe_2P type of structure. At 1473 K the metal atoms are partly disordered. When the sample is slowly cooled, a reverse phase transformation occurs, and below 1363 K the structure is of Co_2P type. Through the transformation, the degree of metal disorder decreases with temperature and tends to zero at 300 K, the Mn atoms selectively occupying the pyramids.

Paramagnetic susceptibility measurements performed on powder samples of the $(Fe_{1-x}Mn_x)_2P$ series with $x = 0.0$, 0.10, 0.20, 0.25, 0.40, 0.50, 0.65, 0.75 and 1.0 are reported here. They permit us to detect the high-temperature crystal transformation within a defined range of composition.

2. Paramagnetic susceptibility

2.1. Experimental details

The samples were prepared in a phosphorus solid–vapour reaction, using mixtures of powdered metal (Fe and Mn purity: 99.9%) and pieces of red phosphorus (99.999%). The starting materials were sealed in an evacuated silica tube and annealed several times at 1070 K. After each annealing, the powder was carefully ground and the degree of crystallisation followed by x-ray scattering using a focusing cylindrical Guinier–Hägg camera ($\lambda_{K\alpha_1}(Cr)$) calibrated with a silicon standard.

Paramagnetic measurements were performed using a conventional Faraday magnetometer calibrated with a sample of Gd_2O_3 (applied magnetic field: 0.8 T). The samples ($\simeq 100$ mg) were sealed under vacuum in small silica sample holders. The applied temperature was controlled in the range 300–1300 K. The samples were all subjected to complete heating–cooling runs between these limits.

2.2. Results and discussion

2.2.1. Phase diagram determination. Preliminary paramagnetic investigations have been performed by Nagase and co-workers [7]. From the paramagnetic behaviour of this system additional information is obtained on the crystal structures. Two sets of $(1/\chi)(T)$ curves were recorded. In the first one, related to the orthorhombic phase ($x = 0.20, 0.25, 0.40, 0.50, 0.65$), a fairly linear thermal dependence is observed up to a temperature T_1, where a sharp anomaly is detected (figure 1). Above this critical temperature, the variation is again linear, almost the same slope. When the temperature is cycled, a hysteresis phenomenon appears whose amplitude depends on the sample composition. If the temperature is lowered to 300 K, the cooling branch of the curve superimposes quite well on the heating one. Several cycles were successively completed and revealed the perfect reproducibility of the results. The upper linear parts of the curves, i.e. for the high-temperature state ($T \geqslant T_1$), were then considered. From these

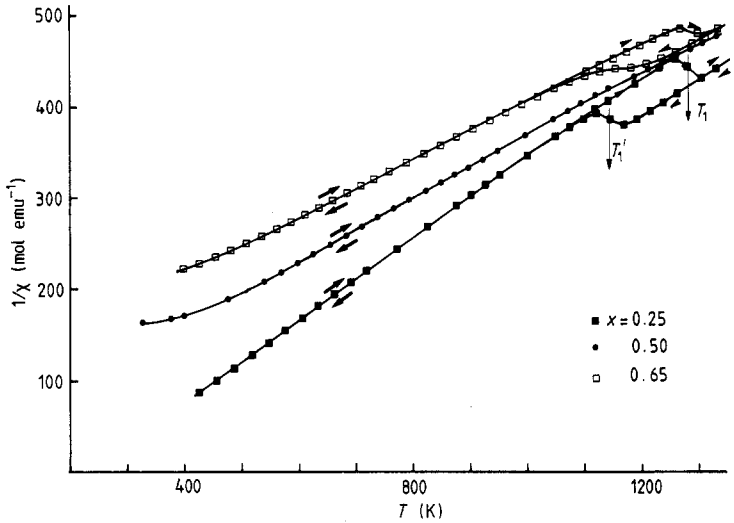

Figure 1. The reciprocal paramagnetic susceptibility for some $(Fe_{1-x}Mn_x)_2P$ compounds: $x = 0.25, 0.50, 0.65$. Before and after the heating cycle, the compounds have O structure.

temperatures different samples were rapidly quenched, and x-ray diffraction analysis performed at room temperature shows that the hexagonal form (H) has been retained.

The second set of $(1/\chi)(T)$ curves is concerned with the hexagonal phases stabilised either via the initial annealing procedure or by quenching from the highest temperature as just described above (figure 2). An upward curvature of the reciprocal susceptibility is systematically observed, but it is reduced as the system nears the limit compound Mn_2P. The curvature is particularly marked for the metastable (quenched) hexagonal compounds, before they transform at $T_2 < T_1$. These quenched solid solutions then exhibit a first-order transition at T_1. After a complete temperature cycle, the magnetic measurements accord with x-ray analysis in showing that initially quenched samples (H_Q) have transformed at T_2 to the orthorhombic structure. Between T_1 and T_2, the heating and cooling curves superimpose on each other (figure 2). The sequence of transformations is schematically represented by

$$H_Q \xrightarrow{T_2} O \xrightarrow{T_1} H \qquad H \xrightarrow{T_1'} O$$

for heating and cooling respectively. Variations with composition of T_1 and T_1' are given in figure 3.

One of the characteristics of the hexagonal series is the upward curvature of the $(1/\chi)(T)$ signal (by comparison with the Curie–Weiss regime observed for the orthorhombic compounds). Since the quenched hexagonal phases are metastable, their reinforced upward curvature of $(1/\chi)(T)$ (by comparison with the H phase) could be attributed to the kinetics of diffusion, approaching the transformation $H_Q \rightarrow O$ at T_2.

The variation of the cell volume per formula unit with the degree of substitution has been analysed, and is reported in figure 4 together with the results obtained in [4] and [6]. Since Fe_2P can be synthesised with the O form [14], the representative curve of the orthorhombic compounds has been linearly extrapolated over the whole domain of substitution. The H- and O-phase curves intersect for low x-values and tend to be parallel for x-values close to 1. The lowest value of x for which the O phase could be spontaneously

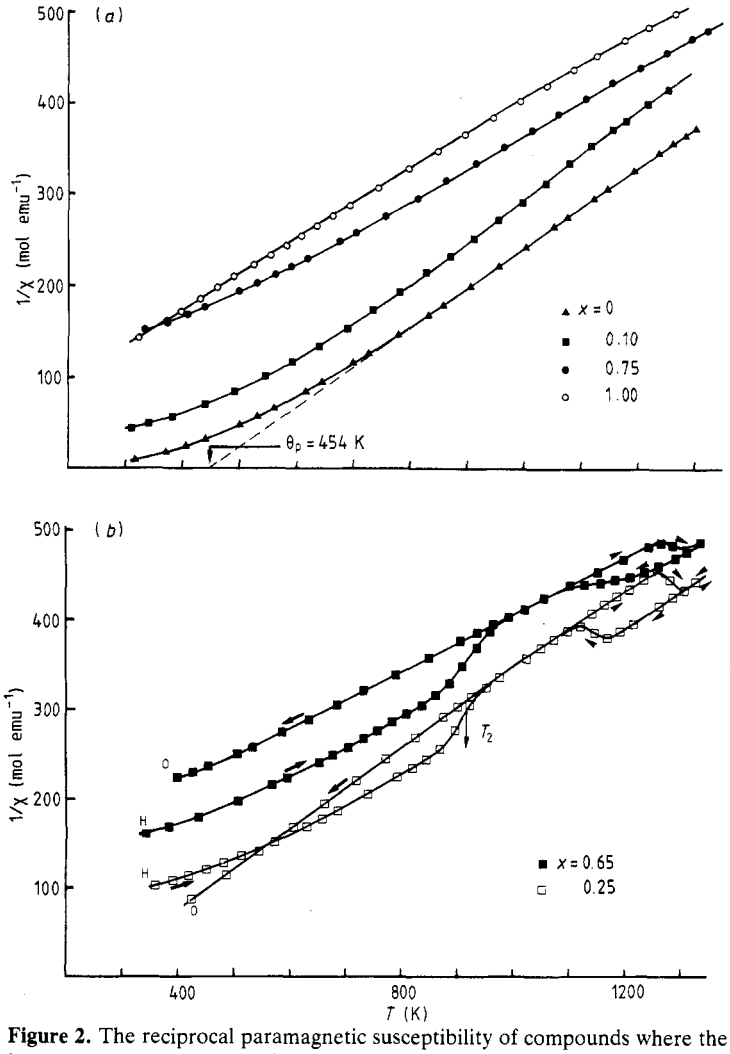

Figure 2. The reciprocal paramagnetic susceptibility of compounds where the initial state has hexagonal symmetry: (*a*) $x = 0.0, 0.10, 0.75, 1.0$ and there is no modification of the symmetry during the heating cycle; (*b*) $x = 0.25, 0.65$.

obtained is $x = 0.12 \pm 0.01$. Since the composition with $x = 0.75$ can only be synthesised with the H form (figure 2), the high-x limit is in the range 0.70–0.75. The discrepancies between the critical x-values, reported in the literature, can be understood by considering the phase diagram for O ↔ H given in figure 3. Because of the hysteresis, the way the samples are cooled from a given temperature is critical.

2.2.2. Structure stability. As already reported in [6], there is a maximum number of Fe–Mn bondings in FeMnP. These bondings are assumed to be the strongest ones. However, the existence of the FeMnP hexagonal phase (at high temperature), involving the same number of Fe–Mn bondings, shows that a simple argument based on the relative strengths of M–M bonds is not sufficient. The stability of the orthorhombic phase could be related to the preferential affinity of Mn and Fe atoms for the pyramidal and tetrahedral sites, respectively: the affinity is satisfied by 50% Mn–50% Fe.

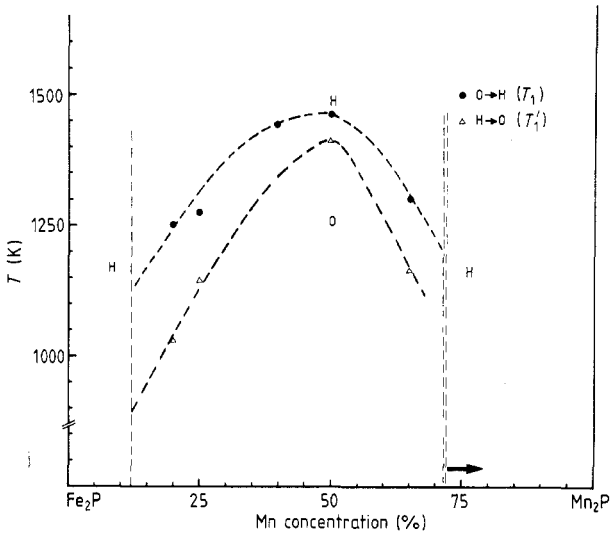

Figure 3. The crystal phase diagram of the system $(Fe_{1-x}Mn_x)_2P$.

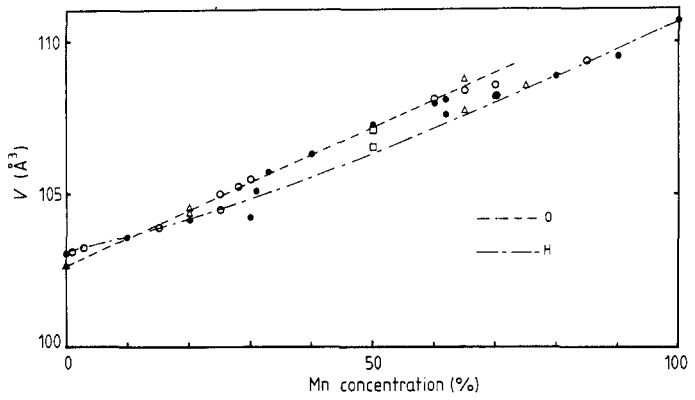

Figure 4. Variations of the cell volume per formula unit versus the degree of substitution in $(Fe_{1-x}Mn_x)_2P$: ●, [4]; ▲, Fe_2P with O structure [14]; ○, [6]; △, *this work*; □, *parameters* obtained for a mixture (H and O).

Using a band model, Goodenough has already suggested that the relative energies of the two phases should depend on the ratio of the energy gained by enhanced metal–metal bonding to the elastic energy lost by lowering the symmetry (from H to O) [15]. The difference in isotropic elastic energy may be simply expressed as [16–18]:

$$\Delta E_{elas} = \Delta V K^{-1}(V_O - V_O(0))^2/2V_O^2(0)$$

where ΔV is the difference $V_H - V_O$ at 300 K between the volumes of three formula units for the hexagonal and orthorhombic cases, $V_O(0)$ is the volume at 0 K of the orthorhombic cell for three formula units, and K is the isothermal compressibility. In the case of Fe_2P with $K = 4.8 \times 10^{-13}\,cm^2\,dyn^{-1}$ [19], calculations provide an estimation of $\Delta E_{elas} \simeq 0.3 \times 10^{-3}$ eV. This small value must be compared with the difference in

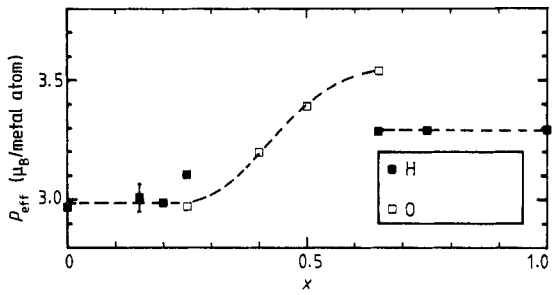

Figure 5. Evolution of the effective magnetic moment p_{eff} in $(Fe_{1-x}Mn_x)_2P$.

energy of the 3d states (≃2.7 eV) involved in the change of the overall symmetry [20, 21]. It seems that the elastic contribution will remain small, probably for any value of x.

For low manganese contents, the hexagonal form can be stabilised due to the lower energy of the 3d band. Large Mn substitutions would tend to shift these levels towards higher energy for which the hexagonal structure is no longer stable, relative to the orthorhombic one. In the Mn-rich composition range, the 3d states would be lowered, since the positions of the energy levels are quite similar in Fe_2P and Mn_2P.

2.2.3. Local environment and magnetic interactions. The determination of the effective paramagnetic moment p_{eff} and of the paramagnetic Curie temperature θ_p was performed by extrapolation to $1/\chi = 0$ from the high-temperature linear part of the $(1/\chi)(T)$ curves. The evolution of the effective magnetic moment displays two main features (see figure 5).

(i) There are critical concentrations corresponding to the structure changes. In the Fe-rich side of composition, p_{eff} varies continuously, which contrasts with the case for Mn-rich compositions, where a discontinuity is observed.

(ii) In the range of stability of the H phase, the effective moment remains almost constant with $p_{eff} \simeq 2.97\ \mu_B$/metal atom in the Fe-rich side and $\simeq 3.29\ \mu_B$/metal atom in the Mn-rich side. For Fe_2P we obtain $\mu_p = 2.1 \pm 0.1\ \mu_B$/Fe atom. In the intermediate O range, p_{eff} increases continuously from 2.97 to 3.54 μ_B/metal atom as the composition is varied from $(Fe_{0.75}Mn_{0.25})_2P$ to $(Fe_{0.35}Mn_{0.65})_2P$.

A plot of the paramagnetic Curie temperature versus x is given in figure 6. For compositions close to $x = 0.5$, the crystal transformation temperature T_1 could not be reached by the magnetic measurement apparatus (>1300 K). Consequently the hexagonal phases close to FeMnP have not been analysed. Apart from this lack of information the other compositions studied give results in good continuity.

Over the whole system θ_p decreases monotonically. For the orthorhombic compounds it is negative for $x > 0.45$ and the drop is marked as $x = 0.65$ is approached. (For O phases θ_p is negative for $x > 0.45$, and seems to diverge near 0.65 ($\theta_p = -296$ K).) For the H phases the decrease is less pronounced, θ_p being slightly negative for $x > 0.75$ ($\theta_p(Mn_2P) = -45$ K).

The discontinuities of θ_p and p_{eff} are associated with the discontinuity of the volume itself. They can also be correlated with the difference between the local environments of the two structures. Figure 7 shows the projection of the two structure types along the shortest cell axis for $x = 0.65$. The intermetallic distances have been deduced from neutron diffraction experiments we have performed at 300 K (table 1). The main feature concerns the variations of distances between Mn atoms located on the pyramidal sites. In the O structure there are two Mn–Mn distances of 2.81 Å and two Mn–Mn distances

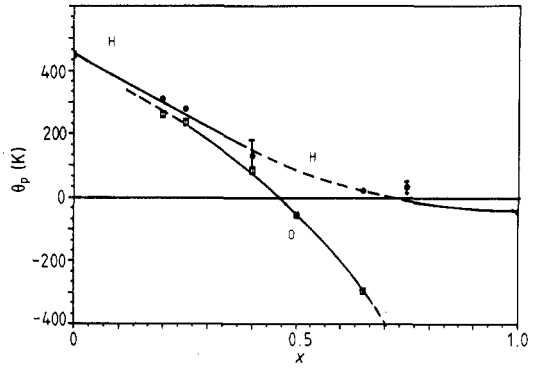

Figure 6. Evolution of the paramagnetic Curie temperature θ_p as a function of both the degree of substitution and the crystallographic phase. The point with $x = 0.4$ has a large uncertainty due to the difficulty of synthesising a single phase by quenching.

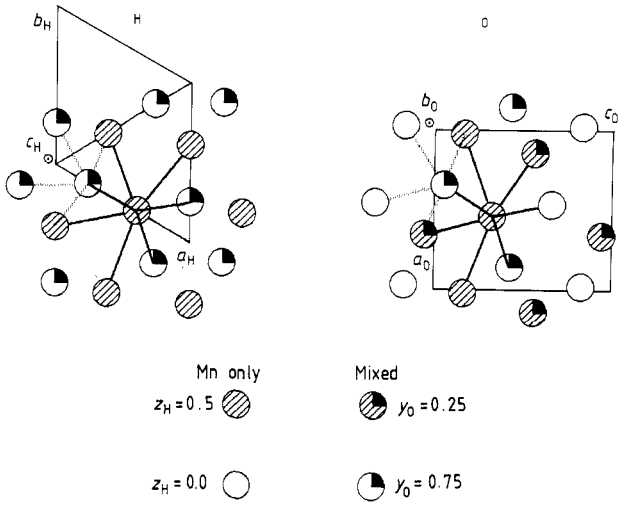

Figure 7. Metal environments in $(Fe_{1-x}Mn_x)_2P$ with either H or O crystal structure for $x = 0.65$.

Table 1. Inter-metallic distances (smaller than 3.4 Å) in $(Fe_{0.35}Mn_{0.65})_2P$ at 300 K for orthorhombic and hexagonal symmetry. The labels pyr and tet refer to pyramidal (100% Mn) and tetrahedral (30% Mn, 70% Fe) sites. The average distances are given in italic type. The cell parameters are in Å: O: $a = 5.981(1)$, $b = 3.582(1)$, $c = 6.774(1)$; H: $a = 5.985(1)$, $c = 3.475(1)$.

	tet–tet	tet–pyr	pyr–pyr
O	2–2.67(2)	1–2.65(3)	2–2.81(3)
		2–2.73(2)	2–3.24(4)
		1–2.81(3)	
		2–2.82(3)	
	2.67(2)	*2.76(2)*	*3.02(3)*
H	2–2.64(1)	2–2.66(1)	4–3.14(1)
		4–2.76(1)	
	2.64(1)	*2.73(1)*	*3.14(1)*

of 3.24 Å that define a tetrahedral environment around the origin atom. In the H case these four distances are equal to 3.14 Å and are distributed in the same (001) plane. Both the distances and the geometry of coordination have been modified. Two Mn–Mn distances have been increased by more than 0.3 Å, away from the value 2.81 Å that has been recognised as a critical value in α–Mn [22]. The change of the exchange interactions with the local environment of pyramidal sites is influenced by the progressive Mn–Fe substitution. For the Mn-rich compounds the substitution for Fe with Mn induces a substantial reduction of the ferromagnetic couplings (figure 6).

Fujii and co-workers have studied by neutron scattering the paramagnetic state of Fe_2P and they have found evidence for strong ferromagnetic correlations persisting up to 775 K, i.e. $T > 3\ T_c$ [23, 24]. This phenomenon was connected to the non-linearity of the $(1/\chi)(T)$ curve. Above 800 K the reciprocal susceptibility displays well a Curie–Weiss-type behaviour. Strong magnetic correlations persisting at such high temperatures can be regarded as an indication of itinerant magnetism [25]. Similar departures of $(1/\chi)(T)$ from a linear regime are found in the system $(Fe_{1-x}Mn_x)_2P$ and appear more pronounced for hexagonal than for orthorhombic compounds. The electrical resistivity behaviour of MM'X compounds (magnitude of the resistivity: about 200 $\mu\Omega$ cm at room temperature) has been studied experimentally and theoretically [19, 26, 27] and is consistent with the itinerant character of the magnetism [28–31].

3. Conclusions

The paramagnetic behaviour of the system $(Fe_{1-x}Mn_x)_2P$ was studied as a function of temperature. From this analysis, crystal structure changes have been pointed out and related to the subsequent modifications of the magnetic correlations.

Definite values for the composition ranges related to the existence of the O or H phase have been proposed. Correlated changes in the local environment of the metal atoms and in the cell volume have been demonstrated at the critical compositions.

The effective magnetic moment has been shown to be dependent on the nature of the metal site, and large changes in the paramagnetic Curie temperature occur over the whole domain of substitution. In the Fe-rich side of the composition the hexagonal phase exhibits strong magnetic correlations up to high temperatures.

These studies show that in the system $(Fe_{1-x}Mn_x)_2P$ the nature of the metal and its local ordering greatly influence not only the magnetic properties but also the stability of the crystal structure.

References

[1] Johnson V and Jeitschko W 1972 *J. Solid State Chem.* **4** 123
[2] Rundqvist S 1962 *Ark. Kemi* **20** 67
[3] Hägg G 1928 *Z. Kristallogr.* **68** 470
[4] Roger A 1970 *Thèse d'état* Orsay University
[5] Fruchart R 1982 *Ann. Chim.* **6+7** 563
[6] Srivastava B K, Ericsson T, Häggström L, Verma H R, Andersson Y and Rundqvist S 1987 *J. Phys. C: Solid State Phys.* **20** 463
[7] Nagase S, Watanabe H and Shinohara T 1973 *J. Phys. Soc. Japan* **34** 908
[8] Fujii H, Hokabe T, Eguchi K, Fujiwara H and Okamoto T 1982 *J. Phys. Soc. Japan* **51** 414
[9] Suzuki T, Yamaguchi Y, Yamamoto H and Watanabe H 1973 *J. Phys. Soc. Japan* **34** 911
[10] Yessik M 1968 *Phil. Mag.* **17** 263

[11] Häggström L, Sjöström J and Ericsson T 1986 *J. Magn. Magn. Mater.* **60** 171
[12] Bacmann M, Chenevier B, Fruchart D and Fruchart R 1988 *Proc. 9th Int. Conf. Solid Compounds of Transition Elements (Oxford) 1988* (Oxford: Royal Society of Chemistry)
[13] Chenevier B, Soubeyroux J L, Bacmann M, Fruchart D and Fruchart R 1987 *J. Solid State Commun.* **64** 57
[14] Sénateur J P, Rouault A, Fruchart R, Capponi J J and Perroux M 1976 *Mater. Res. Bull.* **1** 631
[15] Goodenough J B 1973 *J. Solid State Chem.* **7** 428
[16] Bean C P and Rodbell D S 1962 *Phys. Rev.* **126** 104
[17] De Blois R W and Rodbell D S 1963 *Phys. Rev.* **130** 1347
[18] Nasr-Eddine M and Bertaut E F 1971 *J. Solid State Commun.* **9** 717
[19] Fujii H, Hokabe T, Kamigaichi T and Okamoto T 1977 *J. Phys. Soc. Japan* **43** 41
[20] Ishida S, Asano S and Ishida J 1987 *J. Phys. F: Met. Phys.* **17** 475
[21] Fujii S, Ishida S and Asano S 1988 *J. Phys. F: Met. Phys.* **18** 971
[22] Yamada T, Kunitomi N, Nakai Y, Cox D E and Shirane G 1970 *J. Phys. Soc. Japan* **28** 615
[23] Fujii H, Uwatoko Y, Motoya K, Ito Y and Okamoto T 1988 *J. Phys. Soc. Japan* **57** 2143
[24] Rhodes P and Wohlfarth E P 1963 *Proc. R. Soc.* **273** 247
[25] Wilkinson C, Wäppling R and Ziebeck K R A 1989 *J. Magn. Magn. Mater.* **78** 269
[26] Fujiwara H, Kadomatsu H, Tohma K, Fujii H and Okamoto T 1980 *J. Magn. Magn. Mater.* **21** 262
[27] Chenevier B, Laborde O, Bacmann M, Fruchart D, Fruchart R and Puertolas J A 1988 *J. Phys. F: Met. Phys.* **18** 1867
[28] Eriksson O, Sjöström J, Johansson, B, Häggström L and Skriver H L 1988 *J. Magn. Magn. Mater.* **74** 347
[29] Wohlfarth E P 1986 *Scientific Report UPTEC 86 26 R* (Uppsala: Teknikum Institute of Technology, Uppsala University)
[30] Ishida S, Asano S and Ishida J 1987 *J. Phys. F: Met. Phys.* **17** 475
[31] Fujii S, Ishida S and Asano S 1988 *J. Phys. F: Met. Phys.* **18** 971